Composites Part B 175 (2019) 107086

Contents lists available at ScienceDirect

Composites Part B

journal homepage: www.elsevier.com/locate/compositesb

The effect of cracks on the stability of the functionally graded plates with variable-thickness using HSDT and phase-field theory

Phuc Pham Minh [a], Nguyen Dinh Duc [b,c,d,*]

[a] Faculty of Basic Sciences, University of Transport and Communications, 03 Cau Giay Street, Dong Da, Hanoi, Viet Nam
[b] Infrastructure Engineering Program, VNU Hanoi, Vietnam-Japan University, Luu Huu Phuoc Street, My Dinh 1, Hanoi, Viet Nam
[c] Advanced Materials and Structures Laboratory, VNU Hanoi - University of Engineering and Technology, 144 - Xuan Thuy Street - Cau Giay, Hanoi, Viet Nam
[d] National Research Laboratory, Department of Civil and Environmental Engineering, Sejong University, 209 Neungdong-ro, Gwangjin-gu, Seoul, 05006, South Korea

ARTICLE INFO

Keywords:
Stability
Cracked FGM plate
Variable thickness
New HSDT
Phase field theory

ABSTRACT

In this paper, the stability in a rectangular functionally grade material (FGM) plate with central crack is studied. The plate thickness is changed exponentially following the length of the plate. The properties of the FGM plate are assumed to vary along the thickness direction according to a simple power law distribution. Based on the phase-field theory, the new third order shear deformation plate theory (TSDT) and the finite element method (FEM), the stability of cracked FGM plate is determined. The obtained numerical results are compared with the published articles to ensure credibility. The work also considered effects of changing of the plate thickness ratio, length, crack angle and volume fraction exponent of the functionally graded material on the stability of the plate. Lastly, some visual images of the mechanical instability forms of cracked FGM plates will be introduced.

1. Introduction

Functionally graded materials (FGMs) in plate structures have been developing for such a long time and applicable in many fields of engineering problems due to their outstanding advantages. However, their behaviors during actual using with the consideration of technical effects are still not researched comprehensively. Since the FGMs are popularly applied in extremely severe working conditions such as in great loading or high temperature environment, the structure probably appears defects such cracks. These kinds of failure appearances will weaken strongly the integrity as well as the durability of the structure.

Additionally, it will be easier to make the plate be instable with the effect of cracks when applying the loading compared to the situation of plates that do not have the fractures. Considering the instability problems in plate structures, buckling phenomenon is the most serious behavior due to its unexpected occurrence when the structure suddenly reaches over the highest stress concentration due to a huge thermal or mechanical load applied, then the structure could be made to be in buckling state before reaching to the yield stress state, there is predictable if the capacity of load will be decreased greatly. There are huge numbers of studies in buckling of plate structures. In Yang's study [1], an analysis on buckling is done for FGM plate setting up on the elastic foundation which is modelled based on the formulation of Pasternak. In the research of Thai [2], the principle of Hamilton is applied to derive the constitutive equations for buckling behaviors of the plate which is set on Pasternak foundation. After that, Thai and Kim [3], with the same condition for plate resting on the foundation of Pasternak, an investigation for buckling of FGM plate are presented as a closed-form solution. Numerical method is also used comprehensively in the study of Praveen and Reddy [4], on the basement of the shear deformation plate theory in first order (FSDT), the mechanical behaviors of nonlinear statics and dynamics on the ceramic-metal FGM plate are analyzed by finite element method under a steady temperature and dynamics transverse load conditions. Especially, Reddy [5] has studied the buckling phenomenon of FGM plate with the boundary condition as simple supported using the shear deformation plate theory in higher order. This study has avoided the consideration of the zero transverse shear components at the interface of plate. Yu et al. [6] used a modified Mori-Tanaka and a self-consistent method to study the material properties by modeling the FGMs, Mirzavand et al. [7] studied the thermal buckling of FGM plate that combined with piezoelectric actuators bonded in interface or in the research of Nemat-Alla [8], a 2D-FGM was developed to achieve a better reduction of the thermal stress. Additionally, a new solution for thermal buckling of FGM plate was proposed by Shariat and Eslami [9] in the

* Corresponding author. Advanced Materials and Structures Laboratory, VNU Hanoi, University of Engineering and Technology, 144 Xuan Thuy - Cau Giay, Hanoi, Viet Nam.
E-mail address: ducnd@vnu.edu.vn (N.D. Duc).

https://doi.org/10.1016/j.compositesb.2019.107086
Received 3 February 2019; Received in revised form 17 May 2019; Accepted 1 July 2019
Available online 2 July 2019
1359-8368/

closed-form that they have used the shear deformation plate theory in first order to investigate a thick plate, being similar in using the first order plate theory. Liu et al. [10] proposed a new numerical analysis in buckling of cracked FGM plates by applying both uniaxial and biaxial compression loads, the study used an accurate extended 3-node triangular plate element in the frame of the extended finite element method (XFEM).

Fracture problems such as cracking have an indispensable role in engineering design, analysis, and application, so it is very important to have a useful tool to achieve a well understanding in fracture investigations. Many fracture problems have been modelled by finite element method based on various techniques to treating the cracks. Though the approaches by finite element method have been used extensively, most of the models using finite element method are so fundamental with the virtual crack closure technique [11], or as a remarkable method in modeling fracture, the extended finite element method which is introduced by Moes [12] has also got many focuses from researchers. Nevertheless, these kinds of method still deal with cracking problems in which the cracks are represented discretely and discontinuously, and generally require an explicit and rigorous technique to track the crack path, or need to have applying the strategy of taking average of re-meshing model, in another word, the discontinuities due to the cracking defects are not described well in the model. Phase-field theory is proposed as an advantage method to deal with those problem, it is able to simulate and compute numerically and effectively in both static and dynamic problems such cracking due to its advantages in modeling and analyzing internal fracture in structure such as representing the geometries, shapes and the number of fractures more easily. By applying phase-field method, Duc et al. [13,14] did the exploration of dynamic propagation of cracks in FGM plate, on the other hand, Thom et al. [15] used this method to analyze the effect of various crack's parameters such as size and position in the static instability of FGM plate, after that in another study, he has studied the thermal buckling behavior of cracked FGM plate considering the neutral surface of the plate. The useful applications of phase-field method have been proved in many research, Ulmer et al. [16] applied phase-field approach for a complicated topology of fractures in both plate and shell, Amiri et al. [17] used phase-field method to model the fracture for linear thin shells, Kuhn [18] proposed a continuum phase-field model for different formulations of brittle cracking problem, or Areias et al. [19] used phase-field method in a study of finite-strain plates and shells. In the study of Borden [20], he has demonstrated that phase-field method is able to reduce significantly the implementation complexity in computation process. It is clearly that phase-field method is getting many concentrations from research communities, especially in fracture mechanics field.

Recently, the applications of plate structure with more complicated physical shapes are becoming a new trend in engineering fields. Nonetheless, the negative side of these kinds of structure is that the failure behavior such buckling is more complicated than the flat plate structures, especially with the effect of cracking problems. With the consideration of complex shape such the change of thickness, the buckling phenomenon of plate structure will become much more difficult to understand comprehensively, Duc et al. [21] has demonstrated the effect of the change on plate thickness in a recently study that with a change of plate thickness with 0.05 mm only. According to the best knowledge of the authors, it may be existed several studies in buckling problems of plate structure with variable thickness considering the normal materials of which the material properties are being constant, for example, Phuc et al. [22] has used the Reissner-Mindlin first order shear deformation theory (FSDT) and phase field theory to analyze the buckling behavior of the homogeneous plate with linear variable thickness; however, there has been recently no publication for these investigations of the FGMs problem with the effect of cracks in which the material properties vary according to the thickness of materials. Thus, it is indispensable to study and understand these problems thoroughly.

This paper focuses on an analysis in critical buckling behaviors of FGMs plate having variable thickness with cracking effect using phase field theory for modeling the defects, and the new third order shear deformation theory [24] for modeling the plate structure. The calculated results are compared with the solutions of reference [10, 23,25] to show the high reliability of the proposed computational method. Then, the impact of the variable thickness of the FGM plate on critical buckling values in plate's instability is investigated and discussed in the following sections. The analysis of buckling behavior in ceramic-metal FGM plate with the variable thickness provides very useful information to predict the failure risks in engineering problems, also improves and develops a new computational model in plate structural problems. The second section presents the plate modeling method which is the new third order shear deformation theory, after that, the next section describes the phase-field method applying for crack modeling. The analyses for buckling computations are discussed in the fourth section. Lastly, some conclusions will be summarized in the conclusion section.

2. The third order shear deformation theory of FGM plates with thickness varying according to the x-axis

Functionally graded plates are normally considered to be changing in the material properties following the direction along the plate thickness due to the volume fractions index n. In this study, a specific type of the functionally graded materials (FGMs) is chosen as ceramic-metal P-FGMs plate with a thickness varying according to the x-axis $h(x)$ as described in Fig. 1, supposing that its bottom and top surfaces are being fully composed by metallic and ceramic, respectively. To make the integral numerical computation be easier, the xy-plane is placed to be in the mid-plane of the plate, whereas the positive z-axis is upward from the xy-plane. There are several explanations for the variation of the volume fractions index through the thickness $h(x)$ of the plate, however in this study, the common simple power-law assumption for describing the volume fraction of the ceramic V_c and the metal V_m [1,3–5,7] is being used:

$$V_m = \left(\frac{z}{h(x)} + \frac{1}{2}\right)^n ; V_m = 1 - V_c \text{ with } n \geq 0 \tag{1}$$

With c and m are the ceramic and metal material respectively, z is the thickness coordinate variable with $-h(x)/2 \leq z \leq h(x)/2$, the variable n is signified as non-negative volume fraction gradient index. The Young's modulus E, the Poisson's ratio υ with a power-law distribution as below [1,3–5,7]:

$$E(z) = E_m + (E_c - E_m)\left(\frac{z}{h(x)} + \frac{1}{2}\right)^n, \ \upsilon(z) = \upsilon_m + (\upsilon_c - \upsilon_m)\left(\frac{z}{h(x)} + \frac{1}{2}\right)^n \tag{2}$$

This paper introduces a finite element formulation for functionally graded plate which uses a new simple third-order shear deformation plate theory by Shi [24] based on rigorous kinematic assumption on displacements. It may be due to the fact that the kinematic of displacements is derived from an elasticity formulation rather than the hypothesis of displacements. The three-dimensional displacements (u, v, w) at a point (x, y, z) in the plate can be expressed in terms of five unknown variables as follows:

$$\begin{aligned} u(x,y,z) &= u_0(x,y) + \frac{5}{4}\left(z - \frac{4}{3h^2(x)}z^3\right)\phi_x(x,y) + \left(\frac{1}{4}z - \frac{5}{3h^2(x)}z^3\right)w_{0,x} \\ v(x,y,z) &= v_0(x,y) + \frac{5}{4}\left(z - \frac{4}{3h^2(x)}z^3\right)\phi_y(x,y) + \left(\frac{1}{4}z - \frac{5}{3h^2(x)}z^3\right)w_{0,y} \\ w(x,y,z) &= w_0(x,y) \end{aligned} \tag{3}$$

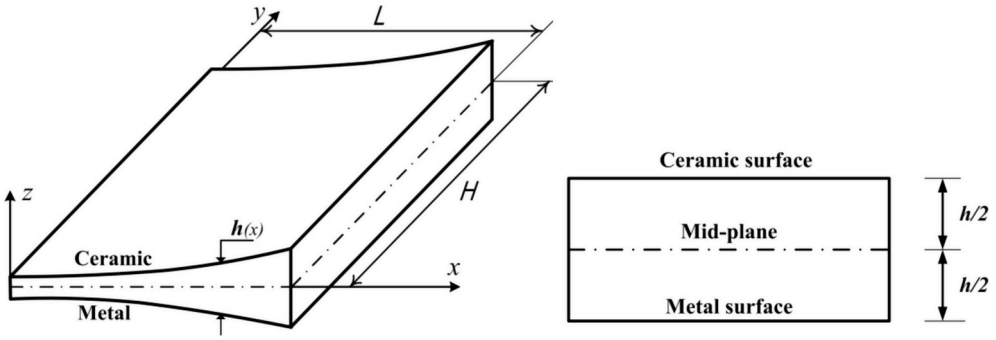

Fig. 1. Geometry of a functionally graded plate with thickness varying according to the x-axis.

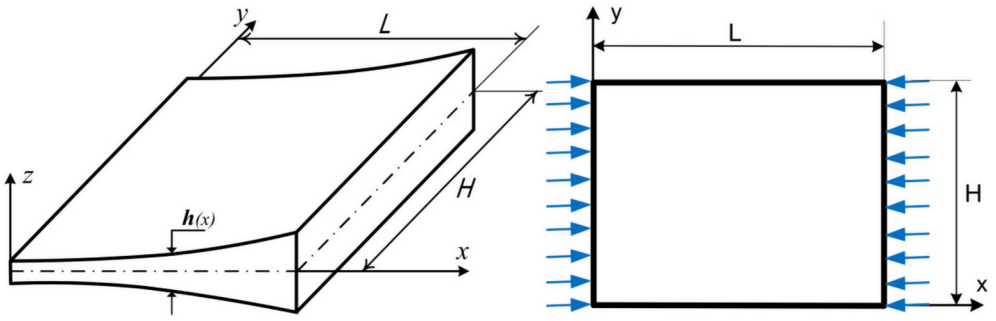

Fig. 2. The non-cracked plate with exponentially varying thickness under uniaxial compression load in x direction.

$$\begin{Bmatrix} \boldsymbol{\varepsilon}_x \\ \boldsymbol{\varepsilon}_y \\ \boldsymbol{\varepsilon}_{xy} \\ \boldsymbol{\gamma}_{yz} \\ \boldsymbol{\gamma}_{xz} \end{Bmatrix} = \begin{Bmatrix} u_{0,x} + z\frac{1}{4}(5\phi_{x,x} + w_{,xx}) + z^3\left(\frac{-5}{3h^2}\right)\left[\phi_{x,x} + w_{,xx} + \left(\frac{-2}{h}\right)h_{,x}(\phi_x + w_{,x})\right] \\ v_{0,y} + z\frac{1}{4}(5\phi_{y,y} + w_{,yy}) + z^3\left(\frac{-5}{3h^2}\right)(\phi_{y,y} + w_{,yy}) \\ u_{0,y} + v_{0,x} + z\frac{1}{4}(5\phi_{x,y} + 2w_{,xy} + 5\phi_{y,x}) + \\ \quad + z^3\left(\frac{-5}{3h^2}\right)\left[\phi_{x,y} + 2w_{,xy} + \phi_{y,x} + \left(\frac{-2}{h}\right)h_{,x}(\phi_y + w_{,y})\right] \\ \frac{5}{4}(\phi_y + w_{,y}) + z^2\left(\frac{-5}{h^2}\right)(\phi_y + w_{,y}) \\ \frac{5}{4}(\phi_x + w_{,x}) + z^2\left(\frac{-5}{h^2}\right)(\phi_x + w_{,x}) \end{Bmatrix} \tag{4}$$

Where u, v, w define the displacements at the mid-plane of a plate in the x, y, z directions respectively. While ϕ_x, ϕ_y represent the transverse normal rotations of the x and y axes. The comma describes the derivative against x and y coordinates.

From the Hooke's law, the relationship of the normal and shear stress with respect to the strains and shear components through the following constitutive equations is given by:

$$\begin{cases} \boldsymbol{\sigma} = \boldsymbol{D}_m(z)\left(\boldsymbol{\varepsilon}^{(0)} + z\boldsymbol{\varepsilon}^{(1)} + z^3\boldsymbol{\varepsilon}^{(3)}\right) \\ \boldsymbol{\tau} = \boldsymbol{D}_s(z)\left(\boldsymbol{\gamma}^{(0)} + z^2\boldsymbol{\gamma}^{(2)}\right) \end{cases} \tag{5}$$

With $\boldsymbol{\sigma} = \begin{bmatrix}\sigma_x & \sigma_y & \sigma_{xy}\end{bmatrix}^T$; $\boldsymbol{\tau} = \begin{bmatrix}\tau_{yz} & \tau_{xz}\end{bmatrix}^T$

$$\boldsymbol{D}_m(z) = \frac{E(z)}{1-v^2(z)}\begin{bmatrix} 1 & v(z) & 0 \\ v(z) & 1 & 0 \\ 0 & 0 & \frac{1}{2}[1-v(z)] \end{bmatrix}; \quad \boldsymbol{D}_s(z) = \frac{E(z)}{2[1+v(z)]}\begin{bmatrix} 1 & 0 \\ 0 & 1 \end{bmatrix} \tag{6}$$

It is necessary to notice that equation (5) are denoted $\boldsymbol{\varepsilon}^{(0)}; \boldsymbol{\varepsilon}^{(1)}; \boldsymbol{\varepsilon}^{(3)}; \boldsymbol{\gamma}^{(0)}; \boldsymbol{\gamma}^{(2)}$ for the strain and shear components induced from equation (4) of displacements in the plate [24].

According to the third order shear deformation theory proposed by Shi [24], the normal forces, bending moments, higher order moments

and shear forces can be computed and written through the following constitutive equations:

$$\begin{Bmatrix} \widetilde{N} \\ \widetilde{M} \\ \widetilde{P} \\ \widetilde{Q} \\ \widetilde{R} \end{Bmatrix} = \begin{bmatrix} \boldsymbol{ABE} & 0 & 0 & & \\ \boldsymbol{BDF} & 0 & 0 & & \\ \boldsymbol{EFH} & 0 & 0 & & \\ 0 & 0 & 0 & \widehat{\boldsymbol{A}} & \widehat{\boldsymbol{B}} \\ 0 & 0 & 0 & \widehat{\boldsymbol{B}} & \widehat{\boldsymbol{D}} \end{bmatrix} \begin{Bmatrix} \boldsymbol{\varepsilon}^{(0)} \\ \boldsymbol{\varepsilon}^{(1)} \\ \boldsymbol{\varepsilon}^{(3)} \\ \boldsymbol{\gamma}^{(0)} \\ \boldsymbol{\gamma}^{(2)} \end{Bmatrix} \tag{7}$$

$$\text{With } (\boldsymbol{A},\boldsymbol{B},\boldsymbol{D},\boldsymbol{E},\boldsymbol{F},\boldsymbol{H}) = \int_{-h/2}^{h/2} (1,z,z^2,z^3,z^4,z^6)\boldsymbol{D}_m(z)dz;\ (\widehat{\boldsymbol{A}},\widehat{\boldsymbol{B}},\widehat{\boldsymbol{D}}) = \int_{-h/2}^{h/2} (1,z^2,z^4)\boldsymbol{D}_s(z)dz \tag{8}$$

$$U(\boldsymbol{\delta}) = \frac{1}{2}\boldsymbol{q}_e^T \int_\Omega \begin{pmatrix} \boldsymbol{B}_1^T\boldsymbol{A}\boldsymbol{B}_1 + \boldsymbol{B}_1^T\boldsymbol{B}\boldsymbol{B}_2 + \boldsymbol{B}_1^T\boldsymbol{E}\boldsymbol{B}_3 + \boldsymbol{B}_2^T\boldsymbol{B}\boldsymbol{B}_1 + \\ + \boldsymbol{B}_2^T\boldsymbol{D}\boldsymbol{B}_2 + \boldsymbol{B}_2^T\boldsymbol{F}\boldsymbol{B}_3 + \boldsymbol{B}_3^T\boldsymbol{E}\boldsymbol{B}_1 + \boldsymbol{B}_3^T\boldsymbol{F}\boldsymbol{B}_2 + \\ + \boldsymbol{B}_3^T\boldsymbol{H}\boldsymbol{B}_3 + \boldsymbol{B}_4^T\widehat{\boldsymbol{A}}\boldsymbol{B}_4 + \boldsymbol{B}_4^T\widehat{\boldsymbol{B}}\boldsymbol{B}_5 + \\ + \boldsymbol{B}_5^T\widehat{\boldsymbol{B}}\boldsymbol{B}_4 + \boldsymbol{B}_5^T\widehat{\boldsymbol{D}}\boldsymbol{B}_5 \end{pmatrix} d\Omega\boldsymbol{q}_e \tag{9}$$

Where $U(\delta)$ is potential energy for plate without of cracks, q_e is used to denote the element displacement vector, δ is displacement vector.

3. Crack modeling and phase field theory

In the phase field theory of fracture mechanics, the description of the state of the material is added with scalar variable s. This scalar variable changes continuously from 0 to 1. When $s = 0$, the material is in a complete cracking state, whereas $s = 1$, the material is in a state of no cracking. If the scalar variable s changes from 0 to 1, the material is in a soft state. Therefore, the scalar variable s describes the state of the material in the cracked region. This scalar variable s is a variable in the strain energy of the plate which is shown in the function s^2, hence when the plate is cracked, the strain energy of the plate decreases.

From the kinematic equation derived above, the total strain energy of plate can be written as:

$$\tilde{\sigma}^0 = \begin{bmatrix} \sigma_x^0 & \tau_{xy}^0 \\ \tau_{xy}^0 & \sigma_y^0 \end{bmatrix} \tag{11}$$

Where σ_x^0, σ_y^0 are the normal stresses in the plate along the x, y axes, respectively; τ_{xy}^0 is the shear stress in the plate on the x – y plane, when external forces acting on the plate.

The first variation of the functional $U(\delta, s)$ according to δ, s is calculated by

$$\begin{cases} \delta U(\delta, s, \delta\delta) = 0 \\ \delta U(\delta, s, \delta s) = 0 \end{cases} \tag{12}$$

From equation (12), the formulations for pre-buckling analyses of cracked plate can be described as follows:

$$\left(\sum \mathbf{K}^e + \lambda_{cr}\sum \mathbf{K}_G^e\right)\delta = 0 \tag{13}$$

$$\int_\Omega 2s\Gamma(\delta)\delta s d\Omega + \int_\Omega 2G_C h\left[-\frac{(1-s)}{4l} + l\nabla s\nabla(\delta s)\right]d\Omega = 0 \tag{14}$$

After finding the value s in equation (14), replacing it on equation (13) could be easily computed the critical buckling load λ_{cr}.

4. Numerical results and discussion

According to the formulations (14) in section 3, the crack shape is defined as the function $\Phi(\delta)$ by Borden [20] as follows:

$$\Phi(\delta) = B\frac{G_C}{4l}.H_0(x,y) \tag{15}$$

$$\text{Where}\quad H_0(x,\ y)\ =\ \begin{cases} \left(1 - \dfrac{d(x,y)}{l}\right) & \text{if } \dfrac{-a\cos\theta}{2} \le x - \dfrac{L}{2} \le \dfrac{a\cos\theta}{2} \\ \end{cases}$$

$$U(\delta,s) = \begin{Bmatrix} \dfrac{1}{2}\boldsymbol{q}_e^T\displaystyle\int_\Omega \begin{pmatrix} \boldsymbol{B}_1^T\boldsymbol{A}\boldsymbol{B}_1 + \boldsymbol{B}_1^T\boldsymbol{B}\boldsymbol{B}_2 + \boldsymbol{B}_1^T\boldsymbol{E}\boldsymbol{B}_3 + \boldsymbol{B}_2^T\boldsymbol{B}\boldsymbol{B}_1 + \\ + \boldsymbol{B}_2^T\boldsymbol{D}\boldsymbol{B}_2 + \boldsymbol{B}_2^T\boldsymbol{F}\boldsymbol{B}_3 + \boldsymbol{B}_3^T\boldsymbol{E}\boldsymbol{B}_1 + \boldsymbol{B}_3^T\boldsymbol{F}\boldsymbol{B}_2 + \\ + \boldsymbol{B}_3^T\boldsymbol{H}\boldsymbol{B}_3 + \boldsymbol{B}_4^T\widehat{\boldsymbol{A}}\boldsymbol{B}_4 + \boldsymbol{B}_4^T\widehat{\boldsymbol{B}}\boldsymbol{B}_5 + \\ + \boldsymbol{B}_5^T\widehat{\boldsymbol{B}}\boldsymbol{B}_4 + \boldsymbol{B}_5^T\widehat{\boldsymbol{D}}\boldsymbol{B}_5 \end{pmatrix} d\Omega\boldsymbol{q}_e + \\ + \dfrac{1}{2}\displaystyle\int_\Omega s^2 \begin{bmatrix} w_{,x} & w_{,y} \end{bmatrix} \tilde{\sigma}^0 \begin{bmatrix} w_{,x} & w_{,y} \end{bmatrix}^T h d\Omega + \dfrac{1}{2}\int_\Omega s^2 \begin{bmatrix} \phi_{x,x} & \phi_{x,y} \end{bmatrix} \tilde{\sigma}^0 \begin{bmatrix} \phi_{x,x} & \phi_{x,y} \end{bmatrix}^T \dfrac{h^3}{12} d\Omega + \\ + \dfrac{1}{2}\displaystyle\int_\Omega s^2 \begin{bmatrix} \phi_{y,x} & \phi_{y,y} \end{bmatrix} \tilde{\sigma}^0 \begin{bmatrix} \phi_{y,x} & \phi_{y,y} \end{bmatrix}^T \dfrac{h^3}{12} d\Omega + \displaystyle\int_\Omega G_C h\left[\frac{(1-s)^2}{4l} + l|\nabla s|^2\right] d\Omega \end{Bmatrix} = \left\{\int_\Omega s^2\Gamma(\delta)d\Omega + \int_\Omega G_C h\left[\frac{(1-s)^2}{4l} + l|\nabla s|^2\right]d\Omega\right\} \tag{10}$$

With q_e is used to denote the element displacement vector, and G_C is used for the critical energy release rate in Griffith's theory and l is a positive regularization constant to adjust the size of the fracture zone.

$$\text{and } \frac{-l}{2} \le y - \frac{H}{2} + \left(x - \frac{L}{2}\right)\tan\ \theta \le \frac{l}{2}0 \qquad \text{else} \qquad .$$

Where the magnitude of the scalar B is $B = 10^3$, L and H are the length and width of the plate respectively, a and θ are the length and the

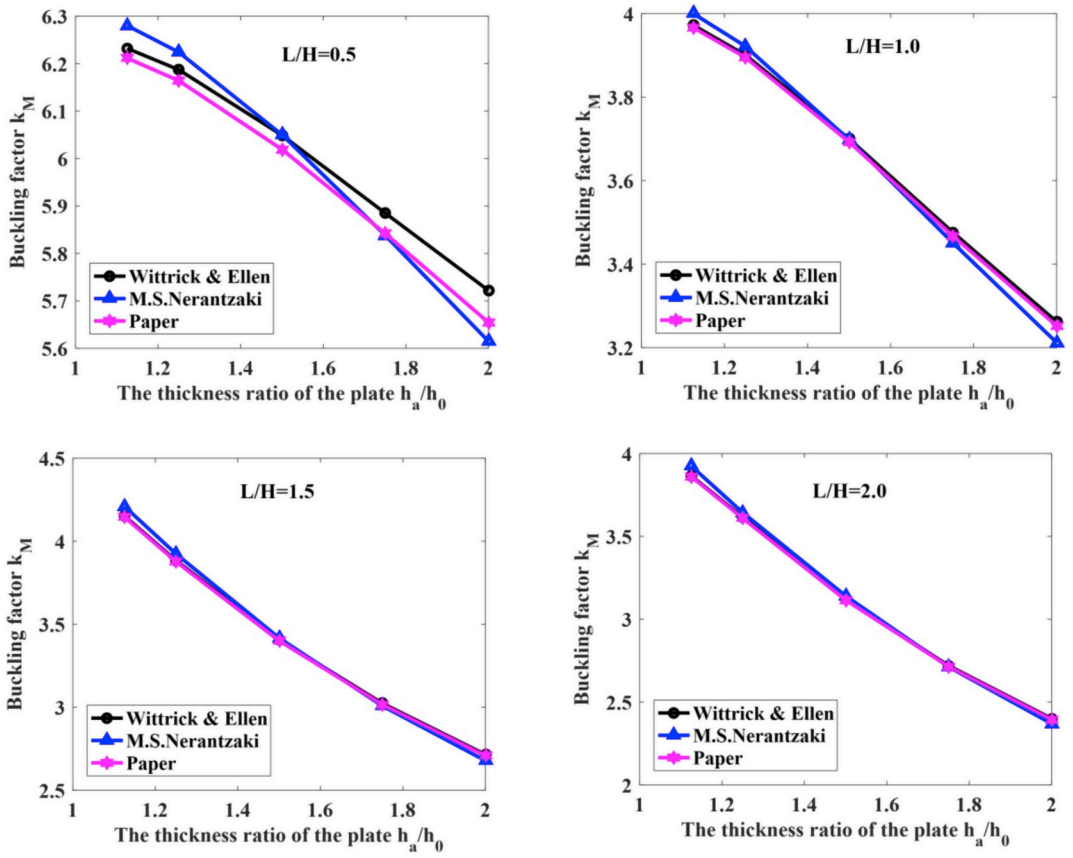

Fig. 3. Comparison of nondimensionalized critical buckling factor of plate subjected to uniaxial compression along the x-axis.

inclined angle of the crack, l is to control the width of the cracking zone, whereas $d(x,y)$ is the closest distance from point (x,y) to the boundary line l in fracture zone. After calculating the value of the function $\Phi(\delta)$ as the crack shape from equation (14), it is possible to find out the phase field variable s, and substitute into equation (13), it is easily to calculate the critical buckling load λ_{cr} and the buckling mode shape δ.

4.1. Buckling factor of uncracked plate with exponentially varying thickness

This study compared the buckling factor of the non-cracked plate with exponential thickness with the results from Refs. [23,25]. Variation in plate thickness is expressed as $h = h_0 e^{\frac{x}{L}\ln\frac{h_a}{h_0}}$. The plate is studied having the length-width ratio $\frac{L}{H} = 0.5;\ 1.0;\ 1.5;\ 2.0$, the thickness of the plate is also adjusted according to the ratio $\frac{h_a}{h_o} = 1.125;\ 1.25;\ 1.5;\ 1.75;\ 2.0$. For convenience in numerical computations, the material properties of plate are set up that the Young modulus $E = 70\ GPa$, Poisson ratio $\upsilon = 0.33$. The analyzing plate has no internal crack, and the plate is compressed in x-axis direction and the boundary condition in the model is set as simple supported in 4 sides (SSSS). Additionally, the buckling factors are calculated as non-dimensional value as following formula [23]:

$$k_M = \frac{\lambda_{cr} H^2}{\pi^2 D_M} \text{ where } D_M = \frac{E h_M^3}{12(1-\upsilon^2)};\quad h_M = \sqrt{h_0 h_a} \tag{16}$$

Fig. 3 shows the buckling factor of plate with the thickness varying exponentially with respect to each dimension of the plate (Fig. 2). It can be observed that the calculated results are almost identical with that of Wittrick [25] and Nerantzaki [23]. When the edge ratio of the plate L/H = 0.5, the buckling factor value is the biggest compared to the remaining cases. This can be explained by the compressive force in the x direction, so the bigger the stiffness in the x direction, the bigger the buckling factor. On the other hand, with H-side constant when the L-side is larger, the stiffness of the plate decreases or in other words, the higher the L/H ratio, the lower the stiffness of the plate.

In all cases, when h_0 is constant, the larger the thickness ratio of the plate h_a/h_0, the faster the local instability for the plate at the thin thickness of the plate (near the thickness position h_0) leads to the smaller the buckling factor.

4.2. Comparison in buckling factor of cracked FGM plate with no change in thickness

The central cracked square FGM plate under compression, as depicted in Fig. 4, is considered in this section. Calculation of stability factors for cracked FGM plate using phase-field theory and third-order shear deformable plate theory is introduced. Plate FGM is made of Al

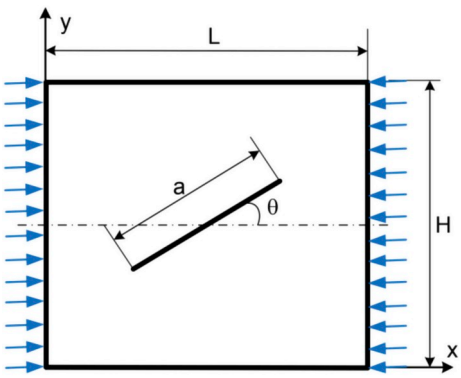

Fig. 4. The square cracked plate subjected to uniaxial compression along the x-axis.

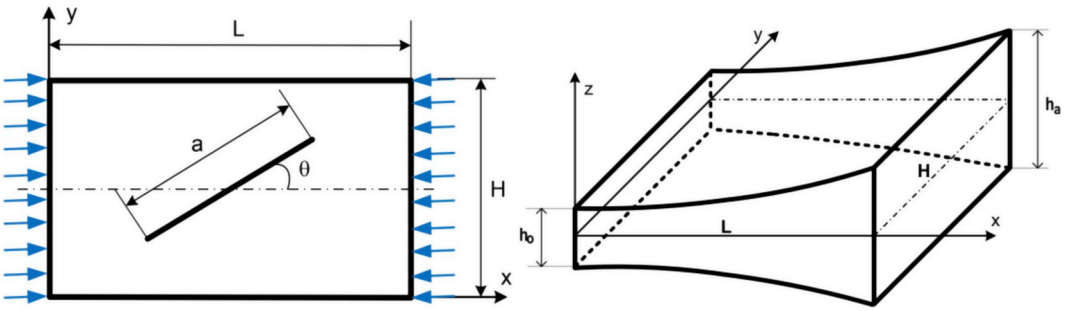

Fig. 5. The rectangular cracked plate with thickness varies exponentially under uniaxial compression load in x direction.

Table 1
Comparison of the buckling factors (k_c) of a square plate FGM with the change of index n and crack length ($L/H=1$; $h/L=0.01$ $\theta = 0^0$).

n	Methods	a/L				
		0.1	0.3	0.5	0.7	0.9
0	XFEM [10]	3.963	3.6273	3.1877	2.8495	2.6807
	Present	3.925	3.5634	3.143	2.8372	2.67
0.2	XFEM [10]	3.5071	3.2105	2.8215	2.5219	2.3723
	Present	3.4877	3.1665	2.793	2.5212	2.3992
0.5	XFEM [10]	3.1001	2.8382	2.4944	2.2295	2.097
	Present	3.0854	2.8013	2.4709	2.2304	2.1225
1	XFEM [10]	2.7709	2.5368	2.2295	1.9927	1.8743
	Present	2.7549	2.5013	2.2063	1.9916	1.8952
2	XFEM [10]	2.5396	2.3246	2.0429	1.8261	1.7179
	Present	2.5235	2.291	2.0207	1.8241	1.7358
5	XFEM [10]	2.356	2.1556	1.8943	1.6936	1.5937
	Present	2.3461	2.1296	1.8782	1.6955	1.6135
10	XFEM [10]	2.2141	2.0256	1.7801	1.5915	1.4977
	Present	2.2116	2.0075	1.7707	1.5983	1.5211

and ZnO_2 with the young's modulus $E_m = 70\ GPa$ and $E_c = 151\ GPa$, respectively. Also, the constant Poisson's ratio of 0.3 is assumed through the thickness ($\upsilon_m = \upsilon_c = 0.3$). Furthermore, the boundary condition in the model is set as simple supported in 4 sides (SSSS). Finally, for analyzing the data, the length of the crack is changed as the ratio with the length of the plate (a/L) with the value of 0.1; 0.3; 0.5; 0.7 and 0.9; and the crack is at the central of the plate with the inclined angle $\theta = 0^0$. The buckling factor of plate is written as follows:

$$k_c = \frac{\lambda_{cr} H^2}{\pi^2 D_c} \text{ where } D_c = \frac{E_c h^3}{12\left(1-\upsilon_c^2\right)}$$

The comparison between current method results and results in Liu's study [10] is described in Table 1, the buckling factors are computed really close with the reference solution. In reference [10], the author has investigated the buckling factors based on the Reissner-Mindlin theory and an accurate extended 3-node triangular plate element in the frame of the extended finite element method (XFEM). In this study, the new third order shear deformation plate theory (TSDT) and the finite element method (FEM) combined with phase field theory in modeling the crack

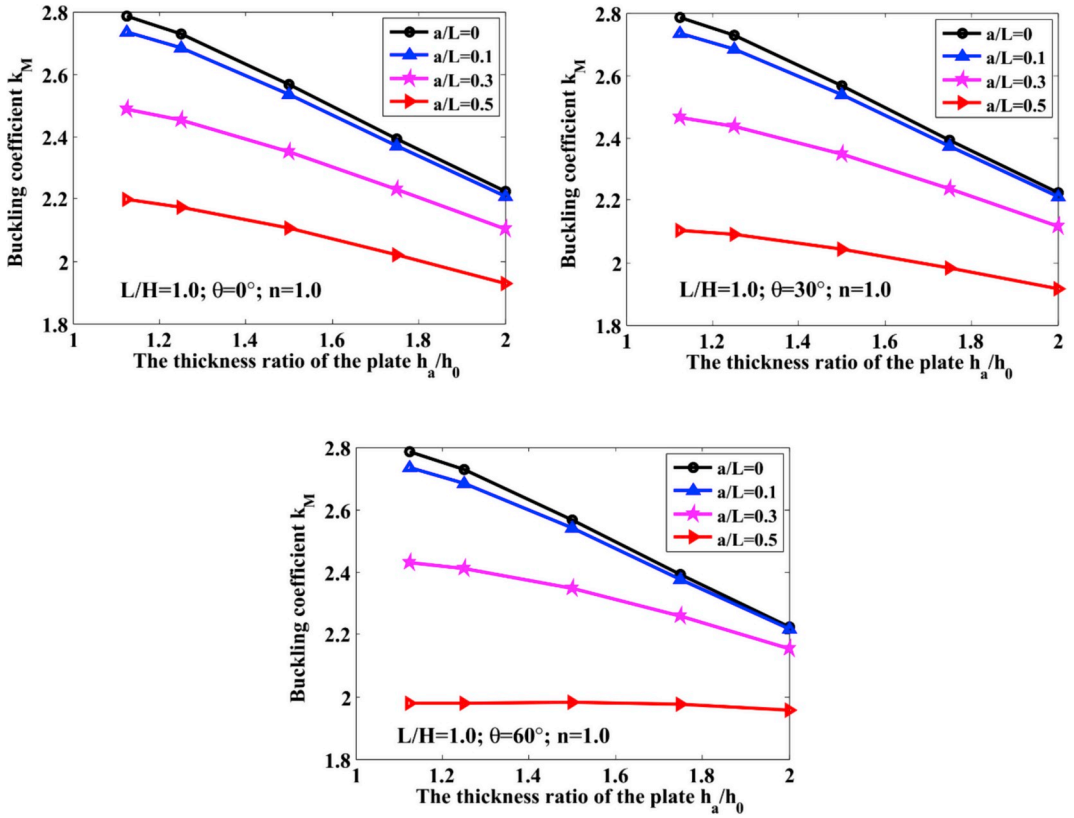

Fig. 6. The effect of cracks on the buckling coefficient of FGM plate with variable thickness.

are used to compute the numerical results of buckling factors, calculated values described in Table 1 are very close to the solutions from the reference.

4.3. The buckling factor of a cracked-FGM plate with the change of thickness

In this section, the buckling factors of cracked FGM rectangular plate with length (L), width H = 0.24 m and variable-thickness follow exponentially along the length of the plate are introduced. The Young modulus and Poisson ratio are kept the same as section 4.2: E_m = 70 GPa;E_c = 151 GPa and $\upsilon_m = \upsilon_c = 0.3$. Otherwise, since the thickness h of the plate is changed exponentially, it can be defined as the formula of $h = h_0 e^{\frac{x}{L}\ln\frac{h_a}{h_0}}$ [23]; where h_0 is the minimum thickness in one side of the plate with $h_0 = \frac{H}{100}$, the thickness h_a of the plate is changed according to the ratio with h_0. Moreover, the crack is analyzed based on the change of length and position, the length (a) of crack will be changed as 0 (no cracks), 10%, 30% and 50% compared to the length (L) of the plate, the crack is in the central of plate with different inclined angles, 0°, 30° and 60°. Finally, the boundary condition of the plate is fully simple support (SSSS) when applying the uniaxial compression load at 2 opposite side following the x axis direction. The numerical results are described in Fig. 6 as follows.

As shown in Fig. 6, cracks are the places that have a significant impact on the stability coefficient of the plate. This is explained by the transformation of energy in the plate. In the plate, there is always a form of energy to be called the potential energy, the crack is the place that releases this energy, which causes the plate to be losed energy and that makes the plate more quickly to be buckling state. In this case, the crack

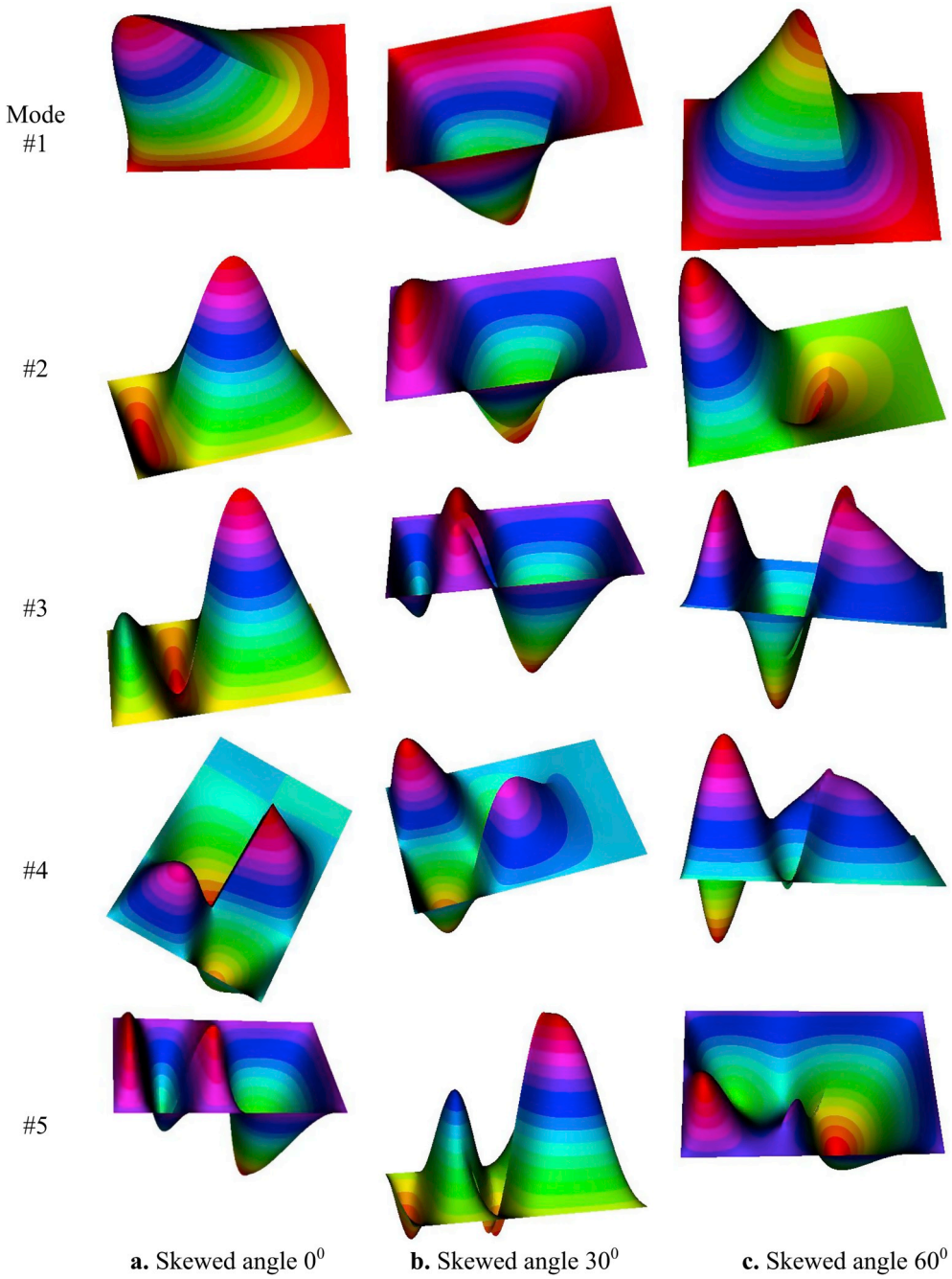

Fig. 7. First five buckling modes of SSSS cracked FGM plate with changing in thickness (L = 0.36 m, H = 0.24 m, $h_a = 2h_0$, n = 2, a/L = 0.5, l/H = 400).

Table 2
Buckling factor k_M of a cracked-FGM square plate with the change of thickness ($L/H = 1$; $h_a/h_0 = 2$) and SSSS.

a/L	θ^0	Gradient index n						
		0	0.2	0.5	1	2	5	10
0	–	3.2593	2.8691	2.5134	2.2246	2.0282	1.8961	1.8028
0.1	0	3.2346	2.8482	2.4957	2.2095	2.0146	1.8831	1.7899
0.3		3.0689	2.7059	2.3742	2.1044	1.9198	1.793	1.7024
0.5		2.8031	2.4748	2.1745	1.9296	1.7615	1.6437	1.5588
0.1	30	3.2387	2.8518	2.4989	2.2124	2.0173	1.8855	1.7923
0.3		3.0836	2.7199	2.3874	2.1167	1.9314	1.8035	1.7118
0.5		2.7711	2.4497	2.1551	1.9145	1.7486	1.6304	1.5445
0.1	60	3.2463	2.8585	2.5048	2.2176	2.022	1.8899	1.7965
0.3		3.1298	2.7624	2.4261	2.1524	1.9642	1.8335	1.7395
0.5		2.8073	2.4895	2.1971	1.957	1.7897	1.6657	1.5737

Table 3
Buckling factor k_M of a cracked-FGM plate with the change of length, angle of inclination ($h_a/h_0 = 1.25$; $a/L = 0.5$; $n = 0.5$) and SSSS.

θ^0	L/H			
	0.5	1	1.5	2
0^0	4.5161	2.4368	2.2144	2.2115
30^0	4.3196	2.3405	2.1553	2.0097
60^0	3.8441	2.2173	2.0659	1.7663

appears in the middle of the plate, which will be the first unstable position due to the compressive force placed at two sides perpendicular to the x-axis. In conclusion, when the length of crack increases, the stability coefficient of the plate will be decreases.

Obviously, the thickness ratio h_a/h_0 of the plate causes greatly affects the stability of cracked FGM plate. The buckling coefficient of the plate is decreased when the thickness ratio is increased, this is explained in section 4.1, because the stiffness of the plate also depends on the thickness of two opposite sides. We also see that the inclined angle of the crack also takes an important role to the stability of the FGM plate. With the inclined angle of the crack is 0°, when h_a/h_0 increases, the buckling coefficient of the plate decreases faster than the case of the inclined angle of the cracks is 30° and 60°. Here, the compressive force is parallel to the x axis, when the inclined angle of the crack is small (the inclined angle of the crack against the compressive force), the crack will be easier for opening with larger area, it means the energy is also more easily released. Hence, the inclined angle of the crack is 0°, the buckling coefficient of the plate is the largest compared to other cases. Therefore, it can be concluded that the difference of thickness between the two sides of the plate or the change of thickness ratio of the plate greatly affects the stability of the plate even more than the impacts from the cracks. Fig. 7 shows the first five shape modes of the buckling in a central cracked rectangular plate when changing the thickness along the length of the plate with the boundary condition of the plate is fully simple support (SSSS).

The next study will assess the impact of the power law index n to buckling behavior in the cracked FGM plate. The length of the central crack is 0; 0.1; 0.3; 0.5 in the ratio with the length of plate is shown in Table 2. The plate is placed as fully simple supported at four sides and is compressed along the x-axis (Fig. 5). The results shown in Table 2 show that, when the power law index n increases then the plate has a high rate of metal composition and thus the stiffness of the plate will be decreased, so the buckling factor decreases.

In Table 3, when the ratio between the edges of the plate increases (L/H), the stability factor of a cracked-FGM plate decreases due to the compressive force along the x-axis. Similarly, when the inclined angle of the crack increases, the stability factor of the plate also decreases.

5. Conclusion

The effect of cracks on the stability of the exponentially variable thickness of FGM plates using high-order shear deformation theory and especially the phase field theory is presented in this study. The high-order shear deformation theory is applied to suit the change thickness of the plate along the x-axis. The phase field theory will be made better in this study because this is the first time it applies to compute internal crack in the FGM plate with variable-thickness follow exponentially. The calculation of the buckling coefficient of the plate has been compared to some reputable paper for checking the reliability of the model. The numerical results show that the change of thickness plate as well as crack parameters significantly affects the buckling coefficient of the plate. Cracking parameters such as length, inclination angle and position of crack change greatly to the buckling coefficient of the plate, when the length of crack increases, due to greater amount of the release energy, the stiffness of the plate decreases, and so the buckling factor decreases. The position of the crack as the middle of the plate also makes instability happen faster than as other locations. When the power law index n increases then the plate has a high rate of metal composition, as a result the buckling factor decreases. The thickness of the plate is changed exponentially, thus the thickness ratio h_a/h_0 greatly affects the stability of the plate. This paper opens a new study in controlling the thickness ratio suitable for changing thickness of FGM plates as well as limiting the force causing instability when the plate appears cracked.

Conflict of interest statement

The authors declare no conflict of interest.

Ackowledgement

This research is funded by Vietnam National Foundation for Science and Technology Development (NAFOSTED) under grant number 107.02-2018.04. The authors are grateful for this support.

References

[1] Yang J, Liew K, Kitipornchai S. Second-order statistics of the elastic buckling of functionally graded rectangular plates. Compos Sci Technol 2005;65:1165–75.
[2] Thai HT, Park M, Choi DH. A simple refined theory for bending, buckling and vibration of thick plates resting on elastic foundation. Int J Mech Sci 2013;73:40–52.
[3] Thai HT, Kim SE. Closed-form solution for buckling analysis of thick functionally graded plates on elastic foundation. Int J Mech Sci 2013;75:34–44.
[4] Praveen GN, Reddy JN. Nonlinear transient thermo elastic analysis of functionally graded ceramic-metal plates". Int J Solids Struct 1998;35:4457–76.
[5] Reddy BS, Kumar JS, Reddy CE, Reddy KV. Buckling analysis of functionally graded material plates using higher order shear deformation theory. J. Compos. 2013. https://doi.org/10.1155/2013/808764.
[6] Yu J, Kidane A. Modeling functionally graded materials containing multiple heterogeneities". Acta Mech 2013. https://doi.org/10.1007/s00707-013-1033-9.
[7] Mirzavand B, Eslami MR. A closed-form solution for thermal buckling of piezoelectric FGM rectangular plates with temperature-dependent properties. Acta Mech 2011;218(1–2):87–101.

[8] Nemat-Alla M. Reduction of thermal stresses by composition optimization of two-dimensional functionally graded materials. Acta Mech 2009;208(3–4):147–61.
[9] Shariat BAS, Eslami MR. Buckling of thick functionally graded plates under mechanical and thermal loads. Compos Struct 2007;78(3):433–9.
[10] Liu P, Bui T, Zhu D, Yu T, Wang J, Yin S, et al. Buckling failure analysis of cracked functionally graded plates by a stabilized discrete shear gap extended 3-node triangular plate element. Compos B Eng 2015;77:179–93.
[11] Krueger R. Virtual crack closure technique: history, approach, and applications. Appl Mech Rev 2004;57(2):109–43.
[12] Moës N, Dolbow J, Belytschko T. A finite element method for crack growth without remeshing". Int J Numer Methods Eng 1999;46(1):131–50.
[13] Duc HD, Tinh BQ, Duc ND, Fazuyoshi F. Hybrid phase field simulation of dynamic crack propagation in functionally graded glass-filled epoxy. Compos B Eng 2016; 99:266–76.
[14] Duc HD, Tinh BQ, Thom VD, Duc ND. A rate-dependent hybrid phase field model for dynamic crack propagation. J Appl Phys 2017;122:115102.
[15] Thom VD, Duc HD, Duc ND, Tinh QB. Phase-field thermal buckling analysis for cracked functionally graded composite plates considering neutral surface. Compos Struct 2017;182:542–6.
[16] Ulmer H., Hofacker M., Miehe C. Phase field modeling of fracture in plates and shells, Proc Appl Math Mech 20102; 12: 171–172.
[17] Amiri F, Milan D, Shen Y, Rabczuk T, Arroyo M. Phase-field modeling of fracture in linear thin shells. Theor Appl Fract Mech 2014;69:102–9.
[18] Kuhn C, Muller R. A continuum phase field model for fracture. Eng Fract Mech 2010;77:3625–34.
[19] Areias P, Rabczuk T, Msekh M. Phase-field analysis of finite-strain plates and shells including element subdivision. Comput Methods Appl Mech Eng 2016;312(C): 322–50.
[20] Borden MJ, Verhoosel CV, Scott MA, Hughes TJR, Landis CM. A phase-field description of dynamic brittle fracture. Comput Methods Appl Mech Eng 2012: 77–95. 217–220.
[21] Duc HD, Thom VD, Phuc MP, Duc ND. Validation simulation for free vibration and buckling of cracked Mindlin plates using phase-field method. Mech Adv Mater Struct 2018;26(12):1018–27.
[22] Phuc PM, Thom DV, Duc DH, Duc ND. The stability of cracked rectangular plate with variable thickness using phase field method. Thin-Walled Struct 2018;129: 157–65.
[23] Nerantzaki MS, Katsikadelis JT. Buckling of plates with variable thickness – an analog equation solution. Eng Anal Bound Elem 1996;18:149–54.
[24] Shi G. A new simple third-order shear deformation theory of plates. Int J Solids Struct 2007;44:4399–417.
[25] Wittrick WH, Ellen CH. Buckling of tapered rectangular plates in compression. Aeronaut Q 1962;13:308–26.